

## **El Chichon: The genesis of volcanic sulfur dioxide monitoring from space**

Arlin Krueger<sup>1</sup>, Nicolay Krotkov<sup>2</sup>, and Simon Carn<sup>1</sup>  
Joint Center for Earth Systems Technology<sup>1</sup>  
Goddard Earth Sciences & Technology Center<sup>2</sup>  
University of Maryland, Baltimore County  
1000 Hilltop Circle  
Baltimore, MD 21250

Corresponding author: [akrueger@umbc.edu](mailto:akrueger@umbc.edu)  
(410) 455 8906  
(410) 455 5868 Fax

### **Abstract**

The 1982 eruption of El Chichon inspired a new technique for monitoring volcanic clouds. Data from the Total Ozone Mapping Spectrometer (TOMS) instrument on the Nimbus-7 satellite were used to measure sulfur dioxide in addition to ozone. For the first time precise data on the sulfur dioxide mass in even the largest explosive eruption plumes could be determined. The plumes could be tracked globally as they are carried by winds. Magmatic eruptions could be discriminated from phreatic eruptions. The data from El Chichon are reanalyzed in this paper using the latest version of the TOMS instrument calibration (V8). They show the shearing of the eruption cloud into a globe-circling band while still anchored over Mexico in three weeks. The measured sulfur dioxide mass in the initial March 28 eruption was 1.6 Tg; the April 3 eruption produced 0.3 Tg more, and the April 4 eruptions added 5.6 Tg, for a cumulative total of 7.5 Tg, in substantial agreement with estimates from prior data versions. TOMS Aerosol Index (absorbing aerosol) data show rapid fallout of dense ash east and south of the volcano in agreement with AVHRR ash positions.

### **Introduction**

In 1982, anomalously high total ozone appeared above Mexico in data from the Total Ozone Mapping Spectrometer (TOMS) on the Nimbus-7 satellite at the same time as the eruption of El Chichon (Krueger, 1983). After 6 centuries of repose, El Chichon erupted violently on March 28 through April 4, 1982. This volcano and the eruptions are well documented in terms of chronology, petrology, stratigraphy, and motion of the ash clouds (Matson, 1983; Robock and Matson, 1983; Varekamp, et al., 1984; Luhr, et al., 1984; Rose, et al., 1984; Sigurdsson, et al., 1984). The detailed behavior of the April 4 eruption gas and ash clouds was analyzed by Schneider, et al., (1999) using data from TOMS and AVHRR instruments.

The TOMS instrument (Heath, et al., 1975, Krueger, 1989), launched in October 1978, was designed, as its name implies, to determine the spatial structure in total ozone through daily, contiguous mapping of the earth. Prior ozone data from ground stations showed high variability with time scales similar to meteorological changes, but the relations with weather were elusive because of the sparse distribution of stations. The

TOMS was built with the best spatial resolution available with 1970's technology (50 km at nadir) to resolve anticipated gradients in total ozone. The spacecraft data rate also limited the spectral coverage to 6 discrete ultraviolet wavelengths for total ozone soundings (Dave and Mateer, 1967). The contiguous mapping proved to be at least as valuable for volcanology as for atmospheric ozone.

The TOMS total ozone algorithm was developed with the assumption that ozone was the only absorbing gas at near UV wavelengths (310 – 380 nm). Other gases were ignored because they were normally present in far lower optical depths than ozone. In 1982, the strange cloud of apparent high total ozone over Mexico (Figure 1) at the time of the El Chichon (small black triangle on Fig. 1) eruption required an explanation. Krueger (1983) showed that the spectral anomalies were consistent with sulfur dioxide, making it the most likely volcanic constituent to account for the anomalous absorption. A simple scheme to separate sulfur dioxide from ozone absorption was proposed. The sulfur dioxide absorption spectrum overlaps the ozone spectrum but with different structure. Other gases, such as carbon disulfide, also absorb at these wavelengths, but would produce different spectral anomalies. Sulfur dioxide amounts were estimated from the deviation of the observed radiances from an interpolation of unperturbed radiances on either side of the volcanic cloud. Agreement at the two TOMS wavelengths within the SO<sub>2</sub> band was within 10%, but absolute amounts were not certain because at the time only room temperature SO<sub>2</sub> cross sections had been measured (Wu and Judge, 1981) while the cloud temperatures were near –50° C. An average column SO<sub>2</sub> amount over the cloud, multiplied by the cloud area obtained from the TOMS images yielded a total mass in the April 5<sup>th</sup> cloud of 3.3 Tg. New cross section data at low temperatures (McGee and Burris, 1987) are now used to produce more accurate results.

With the contiguous coverage and moderate spatial resolution of TOMS it now seemed possible to measure the mass of sulfur dioxide in eruption clouds that were far too large to be assessed from the ground or from aircraft. This began an extended effort to improve the sulfur dioxide retrieval algorithm and to map all of the volcanic eruption clouds in the TOMS database.

The volcanic sulfur dioxide data are derived in part from the standard Level 2 TOMS datasets and in part from special off-line analysis of the Level 1 orbital data. The special analysis is required whenever high sulfur dioxide amounts are present. The retrieval algorithm is implemented in the TOMSPLOT utility software.

### **Volcanic products in TOMS production data**

Three useful products are available for eruption analysis in the standard TOMS output data, available in Level 2 (orbital) format from the Goddard DAAC (McPeters et al., 1993). They include total ozone anomalies, sulfur dioxide index, and aerosol index. Over the years the standard TOMS data production has gone through eight versions as the ozone algorithm and instrument calibration were updated. However, the production algorithm only calculates effective total ozone, as illustrated in **Figure 1a** using the most recent (Version 8) ozone data (Bhartia, et al., 2004). The ozone anomaly due to sulfur dioxide on April 5, 1982 is the irregular red/white area over Mexico. Sulfur dioxide clouds always produce erroneously high total ozone. Thus, even small eruptions may

appear as anomalous bumps in the ozone field, especially in the tropics, where the ozone is nearly constant.

A second useful product is the Sulfur Dioxide Index (SOI), designed for flagging contaminated ozone retrievals (**Figure 1b**). The SOI has been calibrated to yield approximately correct sulfur dioxide amounts for small SO<sub>2</sub> amounts. SOI is the radiance residual at a short TOMS wavelength from the best total ozone solution obtained at a longer wavelength. However, if the ozone is wrong, the residual is wrong. So, SOI is valid only for low SO<sub>2</sub> amounts (< 30 Dobson units). Nevertheless, SOI is a convenient tool for locating volcanic clouds. [NOTE: 1 Dobson unit =  $2.69 \times 10^{16}$  molecules/cm<sup>2</sup>]

A third standard V8 TOMS parameter, Aerosol Index (AI), a residual at a long TOMS wavelength, is a measure of the deviation of the backscattered spectrum from a Rayleigh spectrum. The light scattering properties of the atmosphere at UV wavelengths are dominated by Rayleigh scattering, except when absorbing aerosols, such as volcanic ash, are present. Ash produces large positive AI deviations, shown in red in **Figure 1c** just south of the large white area over the El Chichon sulfur dioxide cloud. Near zero AI values are in green and blue colors. The white areas are invalid retrievals due to the effect of large SO<sub>2</sub> amounts on the ozone retrievals.

The TOMS aerosol index has proved very useful for tracking volcanic ash clouds, which are a hazard to aviation. Other absorbing aerosols, such as dust and smoke, can produce the same signal as ash, so that AI is not unique to volcanic clouds. However, sulfur dioxide is unique to volcanic clouds, so that a combination of the two parameters is a valuable tool for aviation safety.

### **Offline sulfur dioxide retrieval algorithms**

In the original analysis of the El Chichon eruption it became obvious that the TOMS total ozone algorithm could not be used when volcanic clouds were present. In fact, because sulfur dioxide and ozone had similar absorption spectra, it was necessary to solve for both species simultaneously. Jim Kerr of the Atmospheric Environment Service had faced a similar problem with Brewer Spectrophotometer data. He suggested using the Brewer algorithm for the TOMS SO<sub>2</sub> retrievals, adding two other free parameters to account for the scattering properties of the atmosphere and surface. This algorithm was later reformulated as a matrix problem (Krueger, et al., 1995). With ground-based instruments using direct sunlight to measure an overhead absorber the path is simply geometric. The satellite solutions using geometric paths are approximately correct for stratospheric sulfur dioxide clouds but fail with lower altitude clouds.

Satellite-borne observations must consider other factors to determine the path. At UV wavelengths, the paths of photons are rarely geometric; from the sun to the surface and reflected to the satellite, except for snow or ice covered terrain. For more typical low reflectivity surfaces, Rayleigh scattering in the mid-troposphere returns most of the light that is not absorbed by ozone or sulfur dioxide back to space. Absorbers below the scattering layer are only partially sensed. Thus, the optical path must be computed using a multiple scattering radiative transfer model in which the ozone and sulfur dioxide profiles are specified. The ozone profiles are known from climatology, but the sulfur dioxide profiles depend on the eruption style. Explosive eruptions generally reach the

tropopause or lower stratosphere. The path is weakly dependent on altitude above the troposphere so that precise knowledge is unnecessary even for very explosive eruptions that reach the middle stratosphere. Effusive eruptions produce a cloud in the lower troposphere where knowledge of the altitude is more important. However, the path also depends on the total absorber amounts so it cannot be specified before making the retrieval.

An iterative retrieval in which a radiative transfer path is successively approximated was developed as an off-line retrieval method (Krueger, 2000). This makes use of special radiative transfer tables created for volcanic clouds at 5 and 20 km to represent typical effusive and explosive eruption clouds. This retrieval method is implemented in the TOMSPLOT analysis package, available from UMBC as an IDL routine. It was also used to produce the images and total SO<sub>2</sub> mass estimates used in this paper. The iterative retrievals are time consuming, so only regions containing fresh eruption clouds are normally processed this way. Whereas Figures 1- 3 use TOMS standard production data, the following regional figures use the offline Iterative Retrieval data (labeled Iterative SO<sub>2</sub>). Global figures use the standard product SOI (labeled Sulfur Dioxide Index). The figures show the exact ground resolution of the TOMS data by displaying the footprint of each observation.

### **Reanalysis of the El Chichon eruption cloud TOMS data**

The initial El Chichon eruption at 2332 LT on March 28 was observed in GOES infrared image data and tracked every 30 minutes during the course of the eruptions over the next week (Matson, 1984). The IR brightness temperatures were consistent with a plume height above the 16.5 km tropopause. The first post eruption TOMS pass over Mexico at 1816 UT (1216 AM LT) on March 29 showed a significant sulfur dioxide cloud centered NW of the volcano and spreading both east and west (**Figure 2a**). This cloud coincides in part with bright cloud patches in the GOES visible image at 1500 LT (Matson, 1984). The SO<sub>2</sub> cloud has a peak value of 192 DU; the total SO<sub>2</sub> mass in the cloud is about 720 ktons (0.72 Tg). This makes this initial eruption mass greater than the Mt. St. Helens eruption of 1980.

The TOMS AI image shows a large ash cloud had spread northeast from the volcano over the Yucatan peninsula (**Figure 2b**). This cloud coincides with the ash cloud in the GOES visible image. As Matson (1984) notes, the winds at Veracruz were from the southwest between 10.4 and 13.7 km and from the northeast from 20.7 to 24 km. Thus, the winds veered from westerly to easterly from the upper troposphere to the lower stratosphere. Based on the cloud drift the ash was clearly in the troposphere while the SO<sub>2</sub> was in the stratosphere.

On March 30 the previous day's SO<sub>2</sub> cloud center continued to drift slowly northwest and to spread both east and west (**Figure 3a**). This is consistent with a distribution over a range of altitudes such that this plume became sheared into an east – west banner. No new SO<sub>2</sub> was found although a small explosion, possibly phreatic, was reported that morning. No ash cloud remained on March 30, suggesting a rapid fall out due to large particle sizes. The nearly stationary central SO<sub>2</sub> cloud was over central Mexico at a wind minimum near the tropopause; a thinner cloud at higher altitudes

drifted west. On March 31 the high altitude cloud edge had advanced to 140W longitude (**Figure 3b**).

On April 2 a small plume NW of the volcano (**Figure 4**) from renewed activity contained about 17 ktons of SO<sub>2</sub> that was probably due to outgassing because no new eruptive activity has been reported until later that day.

On April 3, a stronger eruption at 0250 LT produced dual clouds that drifted E and NE (**Figure 5a**). These clouds, in the upper troposphere because of the direction of motion, contained about 310 ktons of SO<sub>2</sub>. The eruption also produced a large ash cloud as shown in the AI image (**Figure 5b**), and observed in GOES data Matson (1983). The ash cloud appears south of the sulfur dioxide cloud due to its location in the troposphere.

El Chichon experienced its largest eruption beginning at 0522 LT on April 4. The eruption was detected 6 hours later with TOMS as a great sulfur dioxide cloud centered over the volcano trailing off primarily to the east (**Figure 6a**). Peak SO<sub>2</sub> values were near 600 DU and the mass of SO<sub>2</sub> is at least 3.5 Tg. Some SO<sub>2</sub> may be masked because of the high amounts in the cloud. A large ash cloud is found in the AI image (**Figure 6b**). The position corresponds with that reported by Schneider et al. (1999) from AVHRR data. The ash again is observed primarily south of the SO<sub>2</sub> plume.

The sulfur dioxide cloud center drifted slowly in a northwest direction on April 5 and expanded zonally (**Figure 7a**). The cloud tonnage was 5.6 Tg showing either added SO<sub>2</sub> or unmasking as the cloud spread in area. The peak column amount on April 5 was 330 DU allowing better penetration of UV light to lower altitudes. Ash clouds (**Figure 7b**) are centered SE of the volcano over Guatemala, and widely dispersed from Cuba, to the Gulf of Mexico, over northern Mexico and south over the Pacific Ocean. The Schneider et al. (1999) AVHRR analysis shows agreement with the central ash cloud, but fails to show the dispersed ash.

On April 6 the stratospheric SO<sub>2</sub> cloud separated into three SW- NE trending lobes as it drifted to the west (**Figure 8a**). The lobes correspond to separate volcanic events (Schneider et al., 1999) in which the highest altitude SO<sub>2</sub> is initially carried south by the dynamic perturbation of the eruption. Peak SO<sub>2</sub> amounts (184 DU) continue to drop as the cloud is sheared by the stratospheric winds. The total mass is reduced to 5.2 Tg by conversion to sulfate in the water rich cloud. The ash clouds (**Figure 8b**) are now reduced in area; the densest ash cloud is off the Pacific coast of Guatemala.

On April 7 and 8 the SO<sub>2</sub> cloud lobes elongate and drift westward. The peak values are 132 and 80 DU, respectively. The cloud mass on April 7 is 3.5 Tg. Mass estimates become more difficult as the cloud area increases. A better perspective is gained from a simulated geostationary view from 120° W longitude on April 8 and 9 (**Figures 9a and 9b**). Note the change in scale between the two figures. Here it is clear the volcanic plume extends from Mexico to Hawaii.

### **Global Motion of El Chichon clouds.**

The stratospheric clouds from El Chichon eruptions were carried by easterly winds that varied with altitude from nearly zero at the tropopause to about 22 m/sec at 26 km. The sulfur dioxide band was generally contained within 10 to 30° N as it drifted

across Hawaii on April 8 - 9, crossed the International Date Line on April 10, moved across S. Asia, India, and the Persian Gulf by April 20 (**Figure 10**), then crossed Africa and the Atlantic Ocean before returning to Mexico on April 25 (**Figure 11**). This produced a global-scale banner whose head wrapped around the earth while its tail remained nearly fixed over Mexico. The initially 10 km tall eruption columns were distorted by wind shear into a thin 40,000 km long band in 3 weeks.

A similar banner was observed at visible and IR wavelengths from NOAA operational satellites (Robock and Matson, 1983). Sulfur dioxide does not absorb at these wavelengths so volcanic ash or sulfate from oxidation of sulfur dioxide must be responsible for this signal. The “dust” in the El Chichon cloud was detected in the images by slightly higher reflectivity grays over dark oceans and as a blurring of underlying clouds or surface features.

Both satellite techniques tracked the cloud as it circled the globe, arriving back over Central America on April 25. The leading edge moved 40,000 km west at 22.2 m/sec, but the tail drifted only 1000 km north at 0.55 m/sec. This means that the El Chichon cloud carried a mixture of fine ash, sulfate, and SO<sub>2</sub> at the same altitudes for at least one month. This extraordinary behavior has not been reported from other eruptions. The ash and sulfate aerosols were detected by lidars in Hawaii and Japan. Observers at Mauna Loa saw unusual sunrise and sunsets as early as April 5 and 6. Mauna Loa lidar data showed the appearance of layers of aerosols on April 9 at 22 and 26 km (Coulson, 1983; Deluisi et al., 1983). The 26 km layer was first detected at Fukuoka, Japan on April 18 (Shibata, et al., 1984).

### **Eruption mass**

The initial eruption on March 28 was observed to contain 0.7 Tg SO<sub>2</sub> about 12 hours after its start. Twenty-four hours later the expanding cloud mass was measured at 1.6 Tg. The first cloud was probably too thick for a measurement of the total column so that the second days total is a better measure of the eruption total. Similarly, the major April 4 eruption total is best determined on the second day when a mass of 5.6 Tg was found. The April 3 eruption cloud is relatively dispersed so a mass of 0.3 Tg is realistic. Thus, the cumulative total for all the eruptions on March 28, April 3, and April 4 is 7.5 Tg with an uncertainty of 30% (Krueger, et al., 1995). This mass is substantially higher than the initial estimate (Krueger, 1983) but in good agreement with later estimates using Version 6 of the TOMS calibration (Bluth, et al., 1997; Schneider et al., 1999; Carn et al., 2003).

### **Conclusions**

The 1982 El Chichon eruption was exceeded in mass of sulfur dioxide only by the 1991 Pinatubo eruption during the past quarter century. El Chichon's cloud was unique, anchored near the Mexican source, but stretching westward around the earth in a tropical band that was recognizable in satellite data separately by its sulfur dioxide content and its aerosol content. The leading edge returned just south of the volcano after three weeks; the tropical sulfur dioxide band is recognizable for at least six weeks. This behavior attests to the simplicity of the tropical stratosphere circulation at this time; near zero

winds at the tropopause, increasing uniformly to 22 m/sec at 26 km. This occurred during the Northern Hemisphere Spring season at a time of maximum planetary wave activity, thus demonstrating the great isolation of the tropical atmosphere. The consistency of the sulfur dioxide and ash motion over a month is remarkable and apparently unique to this eruption.

The techniques developed following the El Chichon eruption to discriminate sulfur dioxide from ozone absorption in TOMS data have been applied to all eruptions in the 27 year TOMS database. This quantitative record of volcanic eruption input to the atmosphere removes one of the largest uncertainties in the global sulfur budget.

#### Acknowledgements

The list of research contributors, colleagues, and collaborators is very long. Lou Walters and Charles Schnetzler of NASA GSFC early recognized the geophysical value of the TOMS SO<sub>2</sub> data and encouraged the funding of this work by NASA. Jim Kerr of AES, Toronto, suggested an algorithm for separating SO<sub>2</sub> from ozone used with Brewer spectrophotometer data. This was modified for the satellite environment by the author and Nickolay Krotkov, including suggestions by Pawan Bhartia. Data processing algorithms and software were developed by Scott Doiron, Ian Sprod, Reggie Gallimore, and Colin Seftor. Greg Bluth was the first Post-Doc to analyze data from other eruptions. Near real-time processing methods were developed by Lonnie Bowlin and Bob Farquhar, with the strong encouragement by Mike Comberiate of GSFC and the collaboration of Tom Casadevall of USGS. Tom Simkin and Jim Luhr of the Smithsonian provided conjunctive data for later eruptions. Funding was provided by NASA's Earth Sciences Directorate, including Mike Kurylo, Jack Kaye, and Shelby Tilford, who provided the funding for the follow-on series of TOMS instruments (Meteor-3, ADEOS I, and Earth Probe) that continued the data record until 2006.

#### References:

Bhartia, P.K., et al., Version 8 TOMS Algorithm Theoretical Basis Document, available at [http://toms.gsfc.nasa.gov/version8/version8\\_update.html](http://toms.gsfc.nasa.gov/version8/version8_update.html), 2004.

Bluth, G.J.S., W.I. Rose, I.E. Sprod, and A.J. Krueger, Stratospheric loading of sulfur from explosive volcanic eruptions, *Geology*, 105, 671-683, 1987.

Carn, S.A., Krueger, A.J., Bluth, G.J.S., Schaefer, S.J., Krotkov, N.A., Watson, I.M., and Datta, S. (2003) Volcanic eruption detection by the Total Ozone Mapping Spectrometer (TOMS) instruments: a 22-year record of sulphur dioxide and ash emissions. In Oppenheimer C, Pyle DM, Barclay J (eds) (2003). *Volcanic Degassing*. Geol Soc London Spec Pub 213, 177-203

Coulson, K.L., Effects of the El Chichon volcanic cloud in the stratosphere on the polarization of light from the sky, *App. Optics*, 22, 1036 – 1050, 1983.

Dave, J. V. and C. L. Mateer, A preliminary study on the possibility of estimating total atmospheric ozone from satellite measurements, *J. Atmos. Sci.*, 24, 414-427, 1967.

DeLuisi, J.J., E.G. Dutton, K.L. Coulson, T. L. DeFoor, and B.G. Mendonca, On some radiative features of the El Chichon volcanic stratospheric dust cloud and a cloud of unknown origin observed at Mauna Loa, *J. Geophys. Res.*, 88, 6769-6722, 1983.

Heath, D.F., A.J. Krueger, H.R. Roeder, and B.D. Henderson, The Solar Backscatter Ultraviolet and Total Ozone Mapping Spectrometer (SBUV/TOMS) for Nimbus G, *Opt. Eng.*, 14, 323-331, 1975.

Krueger, A.J., Sighting of El Chichon Sulfur Dioxide with the Nimbus-7 Total Ozone Mapping Spectrometer, *Science*, 220, 1377-1378, 1983.

Krueger, A.J., The global distribution of total ozone: TOMS satellite measurements, *Planet. Space Sci*, 37, 1555-1565, 1989.

Krueger, A.J., L.S. Walter, P.K. Bhartia, C.C. Schnetzler, N.A. Krotkov, I. Sprod, and G.J.S. Bluth. (1995) Volcanic sulfur dioxide measurements from the Total Ozone Mapping Spectrometer (TOMS) Instruments. *J. Geophys. Res.*, 100, 14,057 - 14,076.

Krueger, A. J., S. J. Schaefer, N. A. Krotkov, G. Bluth, and S. Barker, Ultraviolet Remote Sensing of Volcanic Emissions, in *Remote Sensing of Active Volcanism*, edited by P. J. Mouginitis-Mark, J. A. Crisp, J. H. Fink, AGU Geophysical Monograph 116, 25-43, 2000.

Matson, M., The 1982 El Chichon volcano eruptions – A satellite perspective, *J. Volcanol. Geotherm. Res*, 23, 1 – 10, 1984.

McGee, T. and J. Burris, SO<sub>2</sub> absorption cross sections in the near UV, *J. Quant Spectrosc. Radiat. Transfer.*, 37, 165-182, 1987.

McPeters, R.D. et al., Nimbus-7 Total Ozone Mapping Spectrometer (TOMS) Data Products User's Guide, NASA Ref. Pub. 1323, Nov. 1993.

Robock, A. and M. Matson, Circumglobal transport of the El Chichon volcanic dust cloud, *Science*, 221, 195-197, 1983.

Schneider, D.J., W. I. Rose, L.R. Coke, G.J.S. Bluth, I.E. Sprod, and A.J. Krueger, Early evolution of a stratospheric volcanic eruption cloud as observed with TOMS and AVHRR, *J. Geophys. Res.*, 104, 4037 – 4050, 1999.

Shibata, F., Fujiwara, M. and Hirono, M., The El Chichon volcanic cloud in the stratosphere: lidar observation at Fukuoka and numerical simulation, *J. Atm. Terr. Phys.*, 46, 1121 – 1146, 1984.

Varekamp, J.C., J.F. Luhr, and K.L. Prestegard, The 1982 eruptions of El Chichon Volcano (Chiapas, Mexico): Character of the eruptions, ash-fall deposits, and gasphase, J. Volcanol. Geotherm. Res., 23, 39 – 68, 1984.

### **Figure captions**

Figure 1a. TOMS image of total ozone on April 5, 1982 showing anomalous ozone retrievals above Mexico. The anomaly is due to sulfur dioxide absorption at the TOMS total ozone wavelengths.

Figure 1b. TOMS sulfur dioxide index (SOI) on April 5, 1982 from the El Chichon eruption. The red area represents SOI levels above 100 DU.

Figure 1c. TOMS Aerosol Index (AI) image on April 5, 1982 showing a cloud of ash (red) south of the highest El Chichon sulfur dioxide cloud (white).

Figure 2a. The initial El Chichon eruption cloud viewed by TOMS on March 29, 1982.

Figure 2b. TOMS AI image of the March 29 ash cloud drifting NE from El Chichon.

Figures 3a and 3b. Drift of initial eruption cloud to north and west on March 30 and 31.

Figure 4. Small SO<sub>2</sub> plume from El Chichon outgassing on April 2.

Figures 5a and 5b. April 3 SO<sub>2</sub> and ash clouds from 0250 LT eruption

Figures 6a and 6b. The SO<sub>2</sub> and AI (ash) clouds after the 0522 LT eruption on April 4.

Figures 7a and 7b. April 5 sulfur dioxide cloud as it is sheared to the east and west. The ash cloud has drifted over Guatemala and dispersed widely.

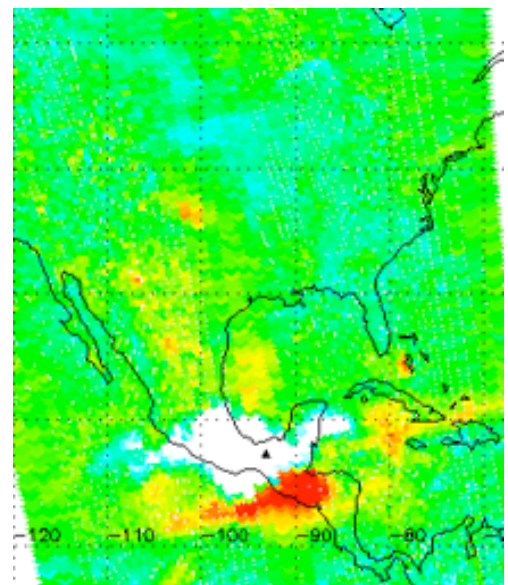
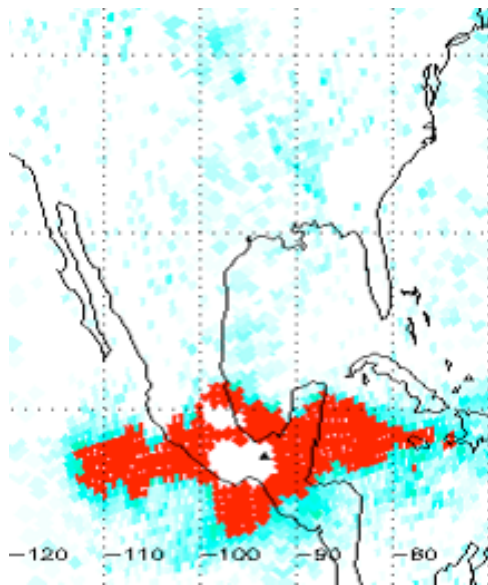
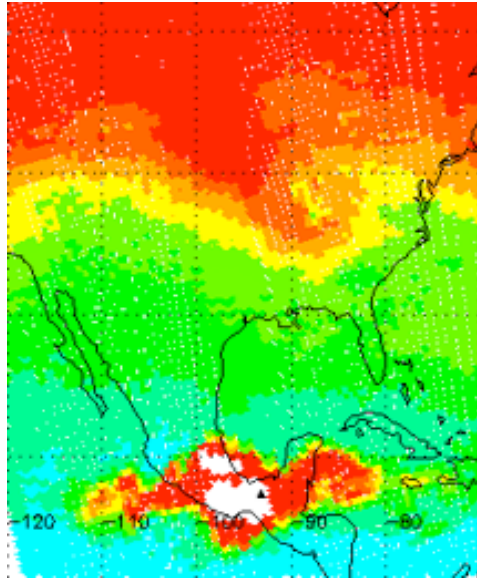
Figures 8a and 8b. April 6 SO<sub>2</sub> cloud has separated into 3 lobes. The ash cloud maximum moved over the Pacific Ocean.

Figure 9a and 9b. Simulated geostationary view of SO<sub>2</sub> clouds drifting west on April 8 and 9, showing arrival of the cloud at Hawaii on April 8.

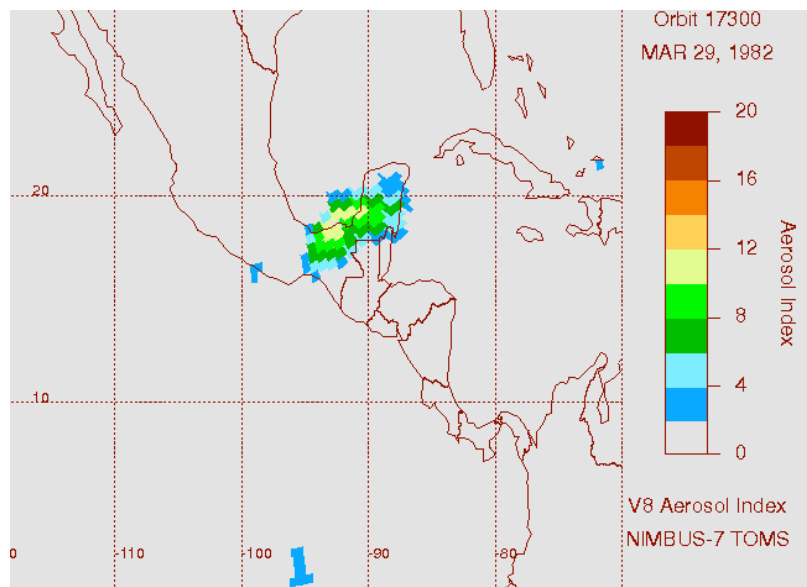
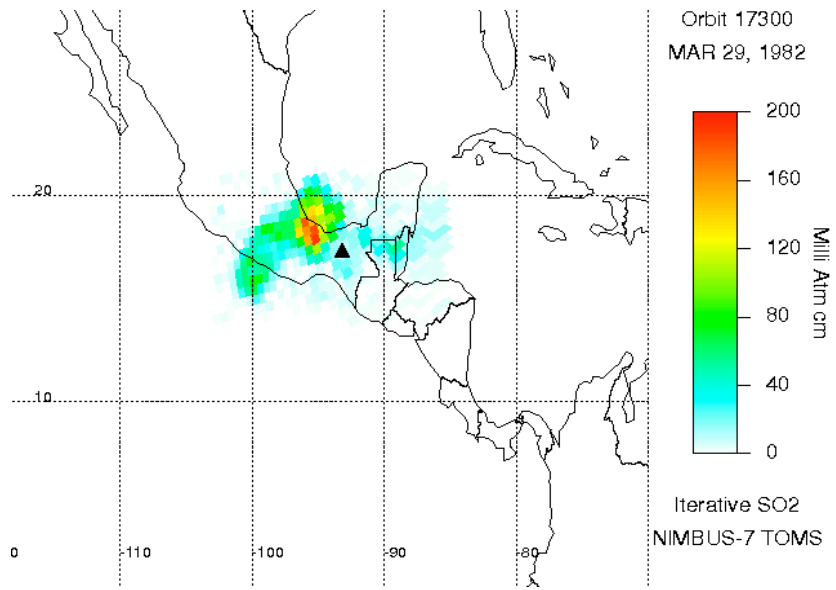
Figure 10. On April 20 the plume has reached East Africa

Figure 11. On April 25 the SO<sub>2</sub> cloud front completed its first global circuit

**Figures:**  
Figures 1a, 1b, and 1c



Figures 2a, 2b



Figures 3a, 3b

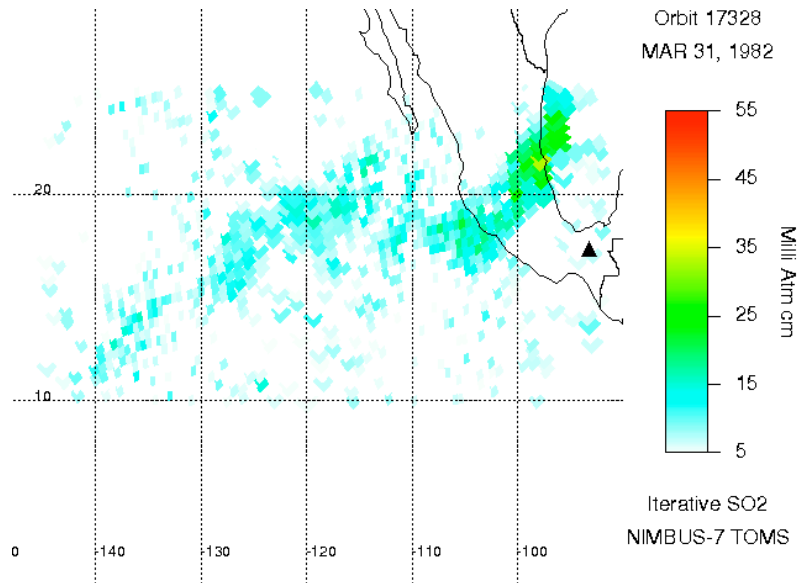
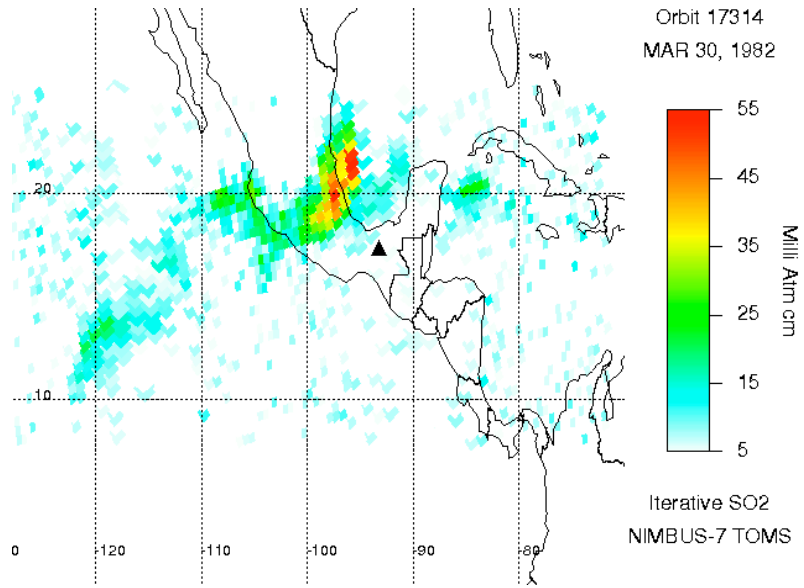
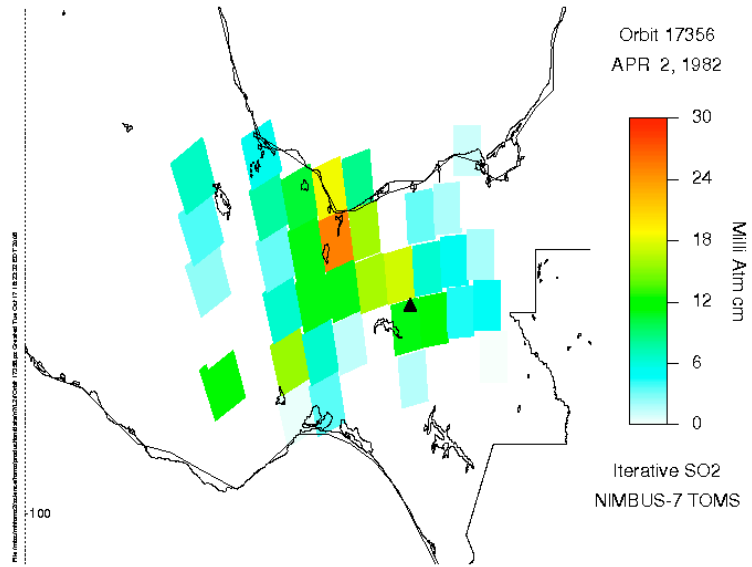
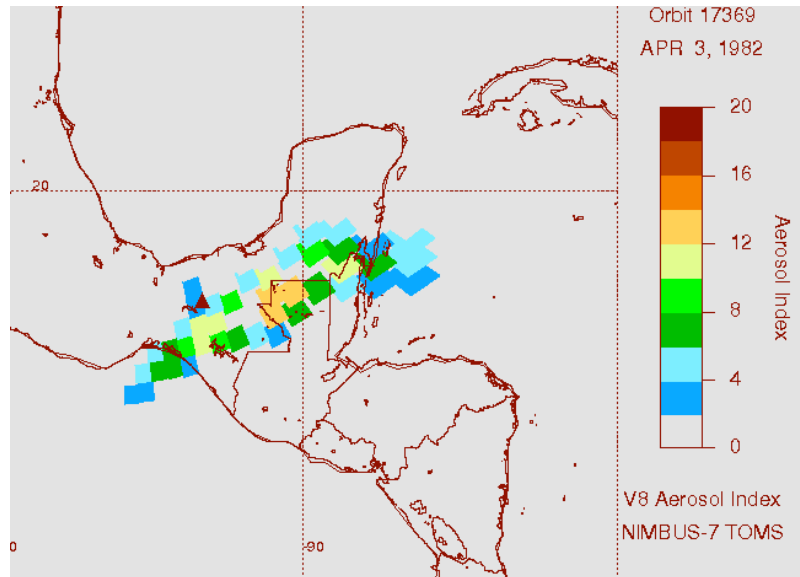
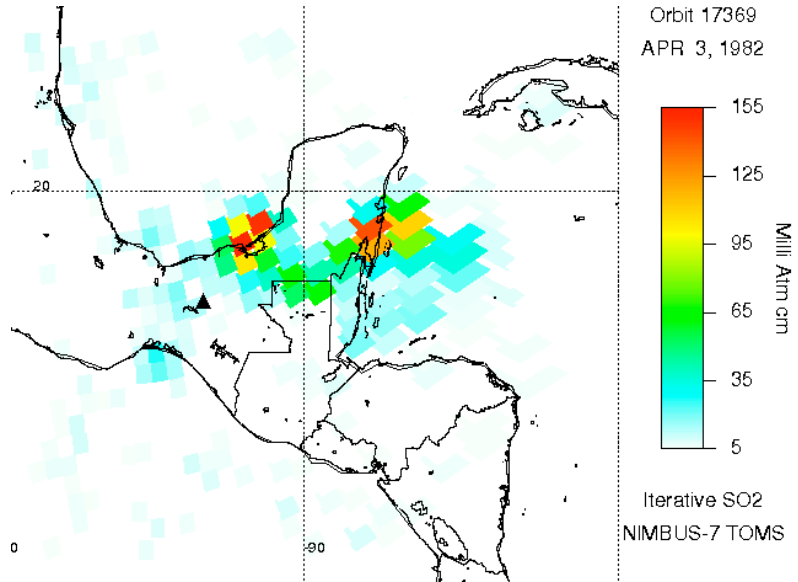


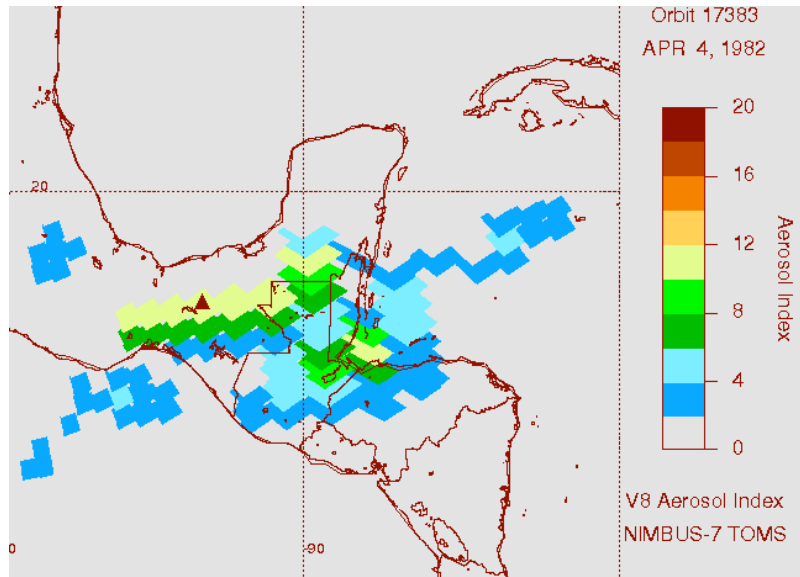
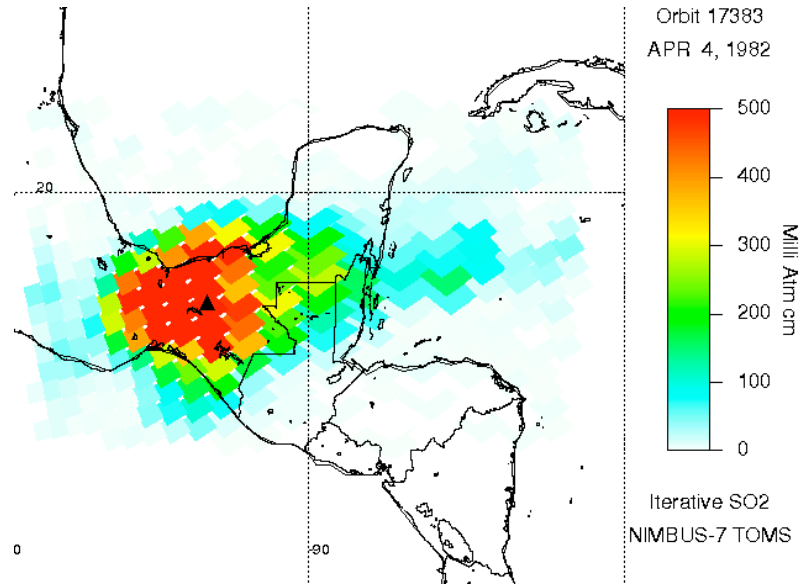
Figure 4



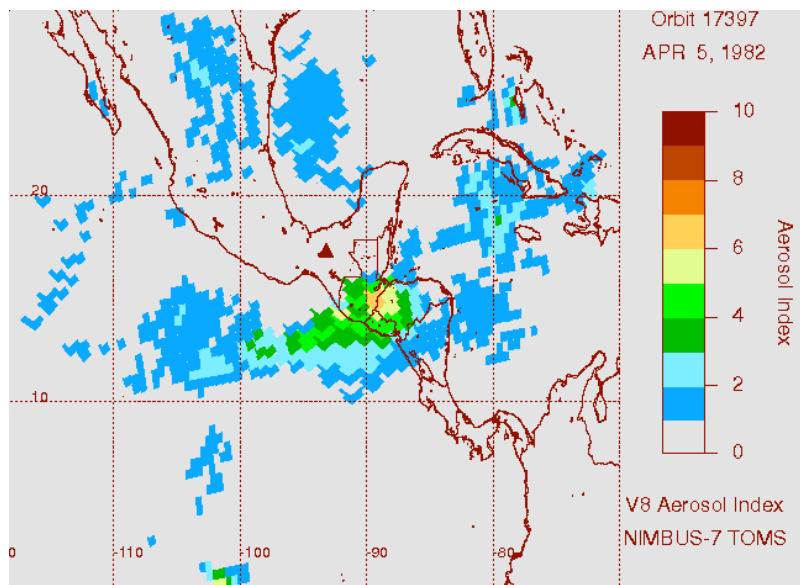
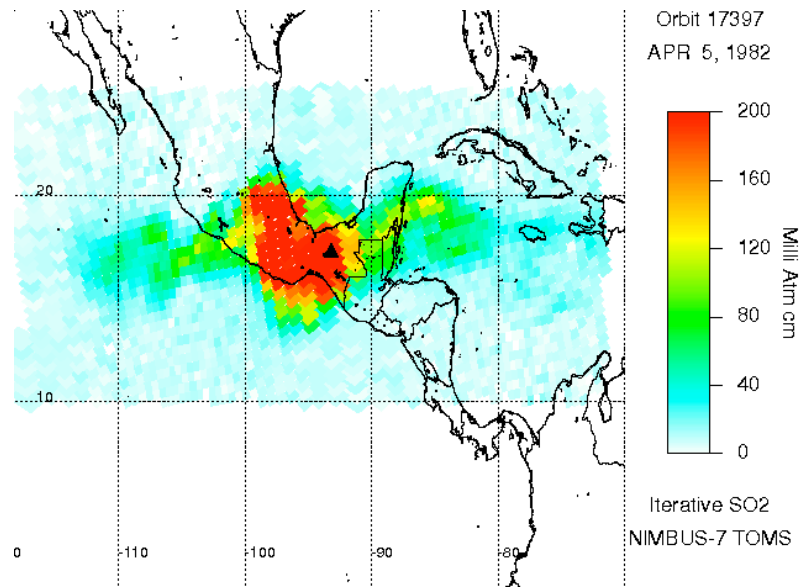
Figures 5a, 5b



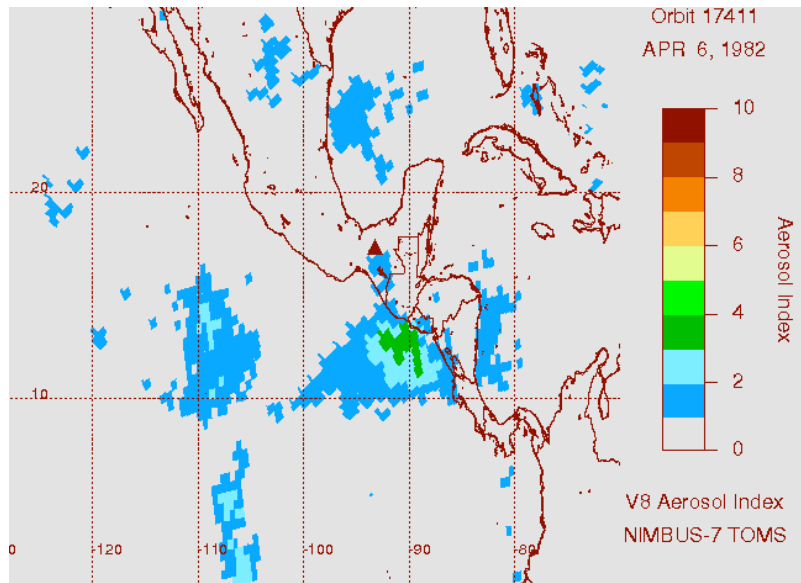
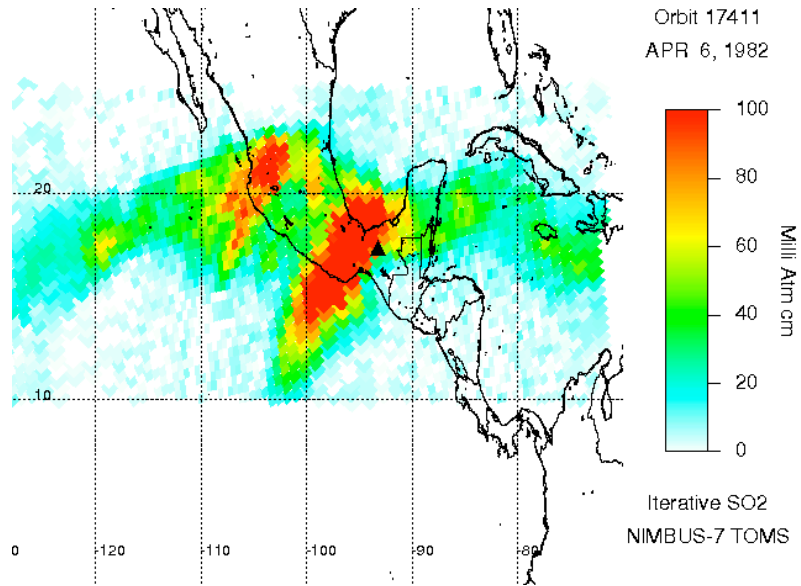
Figures 6a, 6b



Figures 7a, 7b



Figures 8a and 8b.



Figures 9a and 9b. Simulated geostationary view of SO<sub>2</sub> clouds drifting west on April 8 and 9, showing arrival of the cloud at Hawaii on April 8.

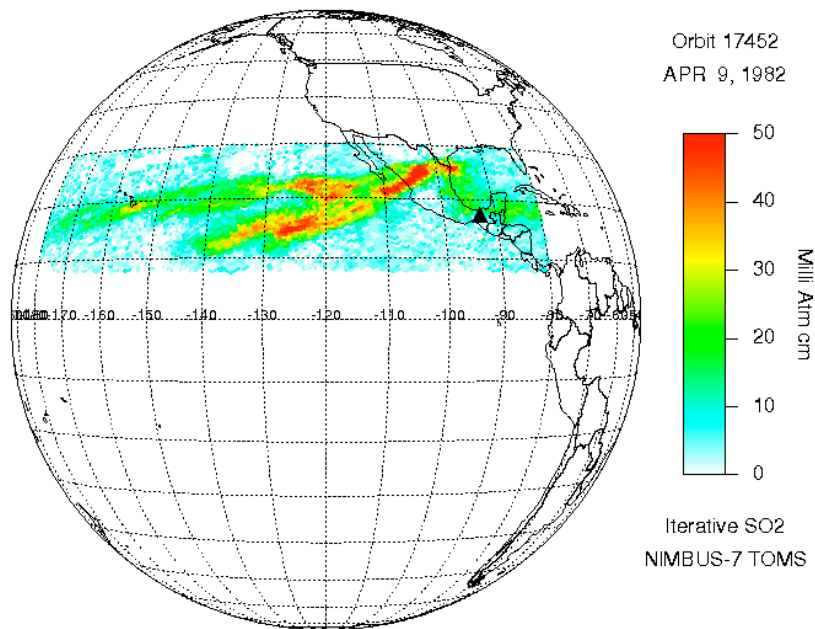
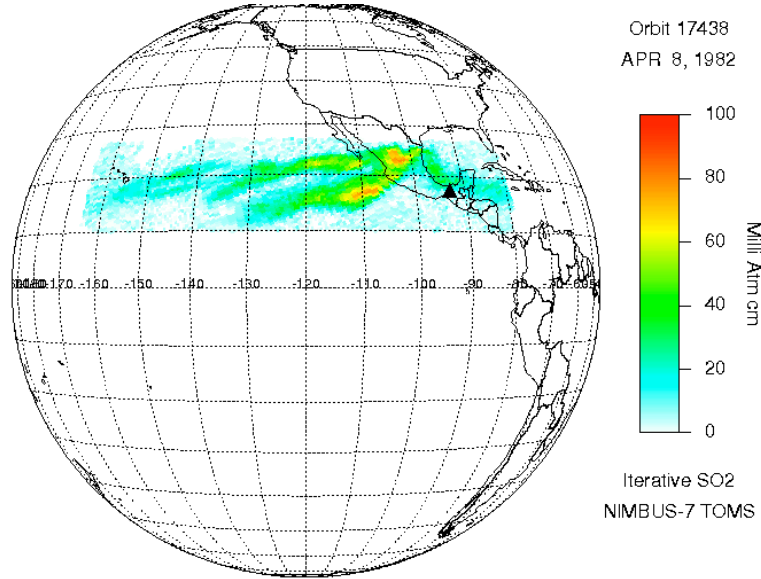


Figure 10. On April 20 the plume has reached East Africa

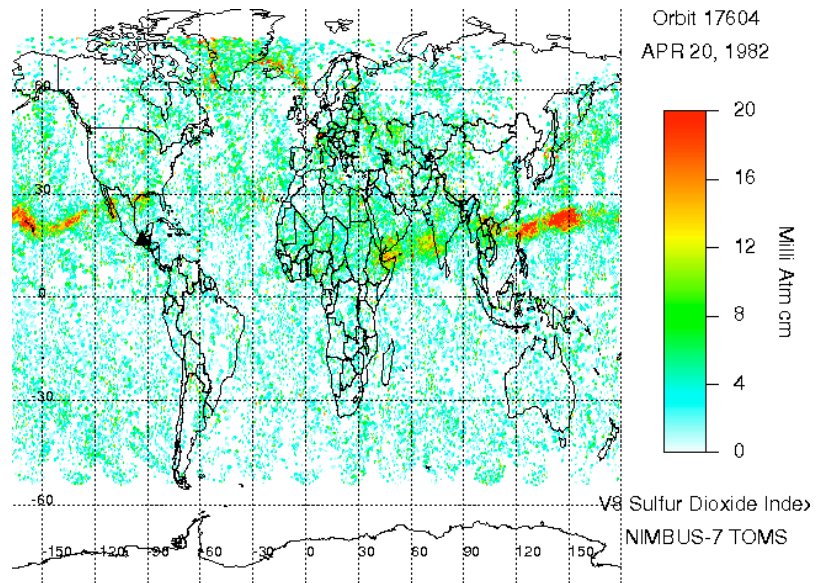


Figure 11. On April 25 the SO<sub>2</sub> cloud front completed its first global circuit.

